Modeling of Dynamic Fragmentation in Brittle Solids

B. Gommerstadt [1] and A. Chudnovsky [2]
[1] Department of Mechanical and Industrial Engineering, Northeastern University, Boston, USA Gommers@coe.neu.edu
[2] Civil & Materials Engineering Department, The University of Illinois at Chicago, Chicago, USA
achudnov@uic.edu

EXTENDED ABSTRACT

Theory of dynamic fragmentation is still under development due to a wide range of applications from the destruction of armor and fracture of oil shale up to the formation of galaxies in the Universe. Dynamic fragmentation of brittle solids is basically influenced by a random flaw nucleation within the body, growth of fracture surfaces, and loading conditions or energy available to drive the fractures. Our efforts to explain fragmentation due to dynamic fracture have focused on consideration of the inherent or induced flaws and its interrelations with the loading conditions, rather than the flaw structure characterization and consider the relationship between statistic and dynamic aspects of the phenomenon and especially the underlying thermodynamic principle appear to play a significant role. In spite of the fact that the famous Griffith criterion based on energy balance does establish the fundamental relationship between energy and flaw size under static loading conditions, there was no conclusive relationships between energy and dynamic fragmentation.

In this communication, we examine two models of dynamic fragmentation (DF) we have proposed previously and make a comparison with experimental data and computer simulations.

The prominent concept based on a description of the energies governing the fragmentation process was proposed by D. Grady [1] in 1982. He derived a simple model of the dynamic fragmentation process in terms of the total free energy of the resulting fragments in an equilibrium configuration. The free energy was taken to be the sum of fragment surface energy, which is created during the formation of new fragment surface area, and a local kinetic energy, which measures the intensity of expansion of the body and is responsible for driving the fragmentation process.

The mean fragment size is obtained by minimizing the free-energy density F with respect to the acquired surface area per unit volume. The fundamental assumption is made that the fragmentation occurs in such a way as to minimize the free energy of the system. A crucial point was the recognition that the total kinetic energy of the body is not available for fragmentation. Only that fraction that is relative to the center of mass can participate in the breakage, while the remainder must continue to reside in the rigid-body flight of fragments. Although good qualitative agreement was obtained with high-rate deformation experiments on such diverse materials as oil shale and steel, in the lower strain rate region the model provides too large fragmentation size.

In our first publication [2] the approach to model dynamic fragmentation based on energy balance was developed. It was done by addition of the strain energy term to the energy balance of the fragment isotropic expansion for three-dimensional liquid or solid. This modest reformulation and a simple extension of Grady's model exhibits the effect of both the elastic energy of the fragment and the local kinetic energy which contribute to the creation of a fragment

The energy balance is:

$$\Delta K_{av} + \Delta F - \gamma A = 0$$

where:

$$\Delta F = \frac{4\pi a^3}{3}\left(\frac{\sigma_*^2}{2K}\right), \qquad \Delta K = \frac{2\pi}{5}\rho\left(\dot{\varepsilon}\right)^2 a^5 \qquad \gamma = \frac{K_{IC}^2}{2\rho C^2}$$

are the potential, kinetic and the surface energy per unit area of new fracture surface, respectively. K is the bulk modulus, ε is the strain rate, and t is the time at which the stress σ reaches the critical value.

Based on the overall energy balance the equation for fragment size a is obtained in [2] as

$$a^3 + \alpha a - 2\beta = 0$$

Here:

$$\alpha = \frac{5}{3}\left(\frac{\sigma_*}{\rho C \dot{\varepsilon}}\right)^2; \qquad 2\beta = \frac{5}{2}\left(\frac{K_{IC}}{\rho C \dot{\varepsilon}}\right)^2$$

The solution of equation (1) is given in [2] and the predictions for the fragment size are shown in Fig. 1 for dense aluminum and in Fig.2 for ceramics. This formula holds for three-dimensional fragment. The one-dimensional counterpart was given in Ref. 6 where the corresponding numerical computations were presented as well.

This model allows one to evaluate an average fragment size for brittle materials with low fracture toughness and a relatively high fracture-initiation stress.

Recent experimental observations [5] and numerical simulations [6],[7] show that this model, or rather the one-dimensional version of it, leads to estimates of fragment size which are in the same order of magnitude than those calculated (in a very wide strain rate region) and measured (in a shorter region). Basically, size predictions based on [2] more consistent than Grady's predictions for low and moderate strain rates, however, in general they still overestimate fragment dimensions. It is clear that fragmentation under quasi-static loading is controlled entirely by the balance between potential and surface energy, in accordance with the theory originally advanced by Griffith [3]. One of the explanations for this inconsistency might be that mutual kinetic-potential energy transformations typical for dynamic processes were ignored in our first approach. On the other hand, this approach as well as Grady's one is based on energy densities consideration and does not contain a flow size. It seams that the model describes pulverization of liquids or comminution of solids rather than fragmentation or disintegration

In our second model [4] we incorporated FM formalism in evaluation strain energy release during fragmentation. The particular mechanism of material disassembling which includes a dynamic interaction of expanding elastic medium with propagating cracks was considered. In particular, we assume also homogeneous dilatation in which no fragmentation occurs until a critical stress, is attained. Crack nuclei are assumed to be homogeneously distributed within the body and, after initiation, the cracks propagate without branching, rotation, kinking, so that the crack length, l, is the only parameter characterizing propagation (and, eventually, fragment size). We specifically exclude any cracks that form by wave-front coalescence.

We also made certain assumptions for simplicity that the ratio of a fragment size to a crack length is equal to one and penny-shaped crack geometry, although, this is by no means required.
At the beginning we apply again the overall energy balance for fragment size, However, in order to calculate the kinetic and potential energy we employ now LEFM theory. Indeed, change in the total mechanical (kinetic and potential) energy W, due to crack growth can be determined as

The energy release per unit crack area for (opening mode cracks) is

$$G_I(dyn) = -\left.\frac{\partial (K + \Pi)}{\partial l}\right|$$

Where $G_I^{(dyn)} = gG_I^{(stat)}$ is the energy release rate for a penny-shaped crack of radius l , and g(v, l) is the so-called velocity factor, which accounts for dynamic effects. It has been found that g is only a weak function of Poisson's ratio and that, to good approximation

$$g(\dot{\ell}) \cong (1 - \frac{\dot{\ell}}{C_R})$$

where C is the Rayleigh wave speed . From the corresponding energy release rate we obtain now

$$\Delta(K + \Pi) = -\frac{(1-\nu^2)}{E} \int_0^{2\pi} \int_0^{\ell} G_I^{(dyn)}(\ell, \dot{\ell})\, \ell\, d\ell\, d\theta$$

where ν is Poisson's ratio, E is Young's modulus.

Substituting these equations into the energy balance we obtain for the constant crack velocity assuming that only half the energy per broken bond at the surface is associated with the given fragment and that a homogenous dilatation of the medium leads to an increase of the stress during the process of crack growth:

$$\ell^3 + \alpha_1 \ell^2 + \alpha\ell - 2\beta = 0,$$

where

$$\alpha_1 = \frac{5}{6}\frac{\sigma_* \dot{l}}{K\dot{\varepsilon}} \qquad \alpha = \frac{5}{27}\left(\frac{\sigma_* \dot{l}}{K\dot{\varepsilon}}\right)^2 \qquad 2\beta = \frac{\pi}{36\, g}\left(\frac{K_{IC}\, \dot{l}}{K\dot{\varepsilon}}\right)^2$$

The only real solution of this equation is obtained in a closed form similar to that in [4]. We omit here the exact algebraic expression for and, instead, present a numerical solution to it in Fig.1.

A large amount of energy is imparted to the body during expansion. The body is not in a state of thermodynamic equilibrium, but tends to reach a state of equilibrium by breaking down. The entropy of the system is increasing and the fragmentation of the body is assumed to occur under an isothermal condition. Energy conservation requires that the total kinetic and potential energy release associated with crack propagation is spent partially on the formation of new surface and is partially dissipated:

$\Delta W - (\Delta K_{av} + \Delta F) = \gamma A + DISS.;\ \Delta F - \Delta W = \Delta\Pi$,

where $DISS = -(\Delta K_{av} + \Delta\Pi + \gamma A)$ is the dissipation. The fundamental thermodynamic assumption is then made that the fragmentation process occurs with minimal dissipation, i.e.,

$$\frac{\partial(\Delta K + \Delta\Pi + \gamma A)}{\partial \ell} = 0$$

Upon substitution of energy terms into this equation it can then be shown to yield the basic equation obtained in [4]:

$$l^3 + 2\sqrt{\alpha}\, l^2 + \alpha l - 2\beta = 0$$

The only real solution of this equation is given in [4] as well. The numerical results for the ceramics are represented in Fig.2.

The LEFM approach permits a unification of previous results, yielding Griffith' solution in the low strain-rate limit and Grady's solution at high strain-rates. We also proposed an extreme energy dissipation principle for evaluation of an average fragment size. This approach presents fragmentation as multiple Griffith' type cracking and predicts the average fragment size at low strain rate to follow from the Griffith condition for brittle fracture, whereas the Grady solution for fluid fragmentation is recovered at a high strain rate. The second model is based on Fracture Mechanics concepts and the assumption that the fragmentation results from multiple cracking. A version of the second law of thermodynamics in the form of extreme dissipation principle has been proposed for evaluation of an average fragment size that led to more adequate treatment of the total energy release rate due to fragmentation. The treatment here does not distinguish or separate between the kinetic and potential energy while in the first model we accounted for both explicitly. This approach unifies both Grady's and our fragmentation models. It presents fragmentation as Griffith' type multiple cracking and it brings prediction of the fragment size at low or zero-strain rate limit into line with the corresponding Griffith's crack size. At the high strain rate limit the Grady solution for fluid is also recovered although in the intermediate strain rate region the fragment size predicted by this FM model significantly depart from Grady's solution and it is smaller than that is in our first model.

Drugan [5] proposed mechanical-based models of fragmentation accounting for the actual time-varying dynamic deformation that occurs prior to fragmentation unset. Fig. 1 compares the predictions of four models: the Grady, Glenn and Chudnovsky (G-C), Glenn, Gommerstadt and Chudnovsky (G-G-C), and the Drugan model (that is assuming initially unflawed material) and the Miller et al. finite element simulations for dense alumina. The results show that the predictions of the two models, G-C and Drugan, tend to converge to Grady's solution at extremely high strain rates. The predictions of the G-G-C model, however, approaching the same 2/3 Grady's slope rather than his asymptote itself. At the quasi-static limit the predictions should correspond to the Griffith solution. At the low strain rates the G-G-C solution reduces to it. However, the G-G-C curve starting, for instance, with the same quasi-static fragment size as Drugan's curve appears to bend at lower strain rates than all the other curves. This behavior is supported by experimental evidence [3], though the data are yet limited to small group of materials.

The dynamic fragmentation of a recently developed hot-pressed silicon carbide, SiC-N, has been studied experimentally by Wang and Ramesh [5] using a modified Kolsky bar technique, together with a servo-controlled hydraulic test machine. High-speed photography was employed to observe and characterize in real-time the evolution of the failure mode and fragmentation during the test. The effect of loading rate for uniaxial loading condition has been measured. It is confirmed that the inertia effect is primarily responsible for the rate effect in the high loading rate regime while subcritical crack growth dominates the effect of loading rate for the low strain rates. As we can see on Fig. 2, the Glenn-Chudnovsky model (as well as Drugan's model would demonstrate) exhibits a transition from the high rate-sensitive area to the insensitive area transitional loading strain rate of around 100000 1/5 , however, the experimental results illustrate that the transitional point is located at around 1000 1/ 5, being close to the transition rate of the compressive

strength. Similar observation agrees also with experimental results on sintered SiC [5]. Prior to this transition rate, the experimental results indicate a moderate rate effect in the corresponding intermediate range while the Glenn-Chudnovsky (and the Drugan's) model exhibits a relatively flat response.

The experimental results [5] on fragmentation size presented on Fig. 2 obviously fall within the prediction ranges of the upper and lower bounds of Glenn-Gommerstadt-Chudnovsky (G-G-C) model, approaching the upper bound more apparent when the stress rate is low and the lower bound when the strain rate is of several hundreds of 1/5. The upper bound was calculated based on maximal possible crack speed for this ceramic material, while the lower bound is computed based on minimal crack speeds of the order of 1/1000 of Rayleigh velocity. The size of fragments in the experiment was determined from the length data of the fragment and the width data of Wang and Ramesh [5] based on fragment volume equivalency.

According to these experimental results, the refined G-G-C model offers more realistic analysis of fragmentation process and the regime of validity of the other models is rather restricted.

Both our models result in estimation of fragment size of the same order of magnitude as observed and calculated by numerical simulations of DF. Further extension of the described approach that includes micromechanical modeling of continuum damage is proposed in this communication. The damage contributes to DF by affecting the rigidity, strength, and toughness of the fragmenting media. Thus, a refined FM based model serves for a better understanding of fragmentation processes and more adequate prediction of the outcome of fragmentation. Application of the above approach in modeling of quasi-static fragmentation resulting from phase and chemical transformation is also discussed.

References

1. Grady D.E., Local inertial effects in dynamic fragmentation, J. Appl. Phys. 53, 322-325 (1982).
2. Glenn, L.A. and Chudnovsky, A., Strain-energy effects on dynamic fragmentation, J. Appl. Phys. 59, 1379-1380 (1986).
3. Griffith, A.A., The phenomenon of rupture and flow in solids, Phil. Trans. Roy. Soc. London, A221:163, 98 (1920).
4. Glenn, L.A., Gommerstadt, B.Y., Chudnovsky, A., A fracture mechanics model of fragmentation, J. Appl. Phys. 59, 1224-1226 (1986).
5. Wang, H. and Ramesh, K.T., Dynamic strength and fragmentation of hot-pressed silicon carbide under uniaxial compression, Acta Materialia 52, 355-367 (2004).
6. Miller, O., Freund, L.B. and Needleman, A., Int. J. of Fracture 96, 101-125 (1999).
7. Drugan, W.J., Dynamic fragmentation of brittle materials: analytical mechanics-based models, J. Mech. & Phys. Solids 49, 1181-1208 (2001).

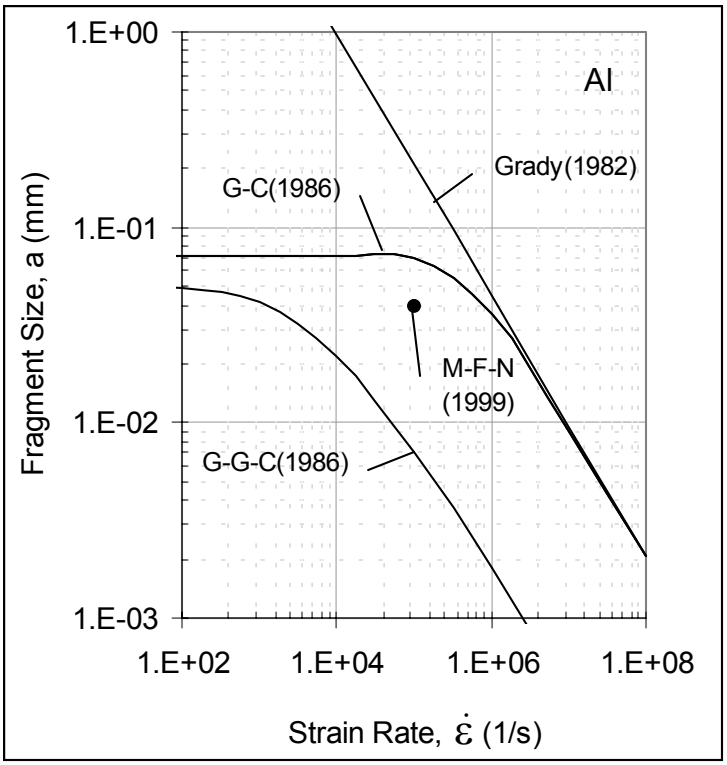
1.E+00
1.E-01
1.E-02
1.E-03
Fragment Size, a (mm)
Al
Grady(1982)
G-C(1986)
M-F-N
(1999)
G-G-C(1986)
1.E+02
1.E+04
1.E+06
1.E+08
Strain Rate, $\dot{\varepsilon}$ (1/s)

Fig. 1

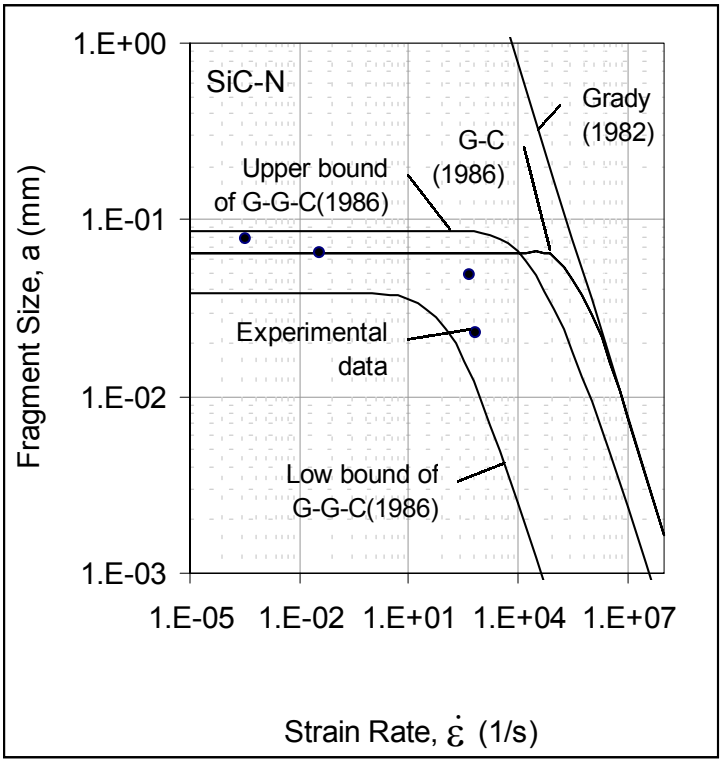
1.E+00
1.E-01
1.E-02
1.E-03
Fragment Size, a (mm)
SiC-N
Grady
(1982)
G-C
(1986)
Upper bound
of G-G-C(1986)
Experimental
data
Low bound of
G-G-C(1986)
1.E-05
1.E-02
1.E+01
1.E+04
1.E+07
Strain Rate, $\dot{\varepsilon}$ (1/s)

Fig. 2